Talanta 134 (2015) 37–47

Contents lists available at ScienceDirect

Talanta

journal homepage: www.elsevier.com/locate/talanta

Fluorometric flow-immunoassay for alkylphenol polyethoxylates on a microchip containing a fluorescence detector comprised of an organic light emitting diode and an organic photodiode

Rong Liu [a], Ryoichi Ishimatsu [a], Masayuki Yahiro [b,c], Chihaya Adachi [a,c], Koji Nakano [a], Toshihiko Imato [a,*]

[a] Department of Applied Chemistry, Graduate School of Engineering, Kyushu University, 744 Motooka, Nishi-ku, Fukuoka 819-0395, Japan
[b] Institute of System, Information Technology and Nanotechnology, 2-1-22 Momochihama, Swawara-ku, Fukuoka 819-0395, Japan
[c] Center for Organic Photonics and Electronics Research (OPERA), Kyushu University, 744 Motooka, Nishi-ku, Fukuoka 819-0395, Japan

ARTICLE INFO

Article history:
Received 16 September 2014
Received in revised form
21 October 2014
Accepted 24 October 2014
Available online 4 November 2014

Keywords:
Organic light emitting diode (OLED)
Organic photodiode (OPD)
Fluorescence immunoassay
Microfluidic
Resorufin
Alkylphenol polyethoxylates

ABSTRACT

A compact fluorescence detector was constructed on a microchip from an organic light emitting diode (OLED) as the light source and an organic photodiode (OPD) as the photo-detector and was used in an immunoassay for alkylphenol polyethoxylates (APE). The OLED based on a terbium complex emitted a sharp light at the main wavelength of 546 nm with a full width at half maximum of 9 nm. The incident photo-to-current conversion efficiency (IPCE) of the OPD fabricated with Fullerene 70 (C_{70}) and tris[4-(5-phenylthiopen-2-yl)phenyl]-amine (TPTPA) was approximately 44% for light at a wavelength of 586 nm. The performance of the fluorescence detector was evaluated for the determination of resorufin (λ_{em}=586 nm) and the photocurrent of the OPD due to the fluorescence of resorufin was proportional to the concentration of resorufin in the range from 0 to 18 μM with a detection limit (S/N=3) of 0.6 μM. The fluorescence detector was successfully utilized in a competitive enzyme-linked immunosorbent assay for APE, where an anti-APE antibody was immobilized on the surface of the channel of the Polydimethylsiloxane (PDMS) microchip or on the surface of magnetic microbeads. After an immunoreaction with a sample solution of APE containing a horse radish peroxidase (HRP)-labeled APE, the fluorescence of resorufin generated just after introduction of a mixed solution of Amplex Red and H_2O_2 was measured using the fluorescence detector. The calibration curve for the photocurrent signals of the OPD due to the fluorescence of resorufin against the logarithmic concentration of APE was sigmoidal in shape. The detection limits defined as IC_{80} were ca. 1 ppb and ca. 2 ppb, respectively, for the methods using the anti-APE antibody immobilized on the surface of the microchannel and in the case where the antibody was immobilized on the surface of magnetic microbeads.

1. Introduction

APE is one of the most widely used surfactants in daily life and is used in a wide variety of industrial processes. When APE is discharged into environmental waters, it can bind to soils and sediments and bioaccumulate in plants and animals [1]. APE and its biodegraded compounds have been suspected to function as endocrine disrupting chemicals. The concentration of APE in water is, by law, restricted less than 20 ppb by the Ministry of Health, Labor and Welfare in Japan [2]. Therefore, a sensitive analytical method for the determination of APE is strongly desired, especially in areas that contain discharge from waste-water-treatment plants. Numerous methods have been proposed for the determination of APE, including gas chromatography [3], liquid chromatography [4] and mass spectrometry [5]. Because of its sensitivity and selectivity, a method based on an enzyme-linked immunosorbent assay (ELISA) [6] by spectrophotometric, fluorimetric or chemiluminescence detection has been widely used for the determination of APE. Zhang et al. reported on a chemiluminescence immunoassay based on a sequential injection analysis (SIA) using magnetic microbeads for the determination of APE with detection limit as low as IC_{80} is ca. 10 ppb [7]. However, as far as we know, including our previous research, attempts to combine ELISA with fluorometry using an OLED and an OPD are limited. Ishimatsu et al. reported on a fluorimetric immunoassay for APE based on a flow injection analysis (FIA) system equipped with a fluorescence detector using an OPD and magnetic microbeads. They achieved a

* Corresponding author. Tel./fax: +81 92 802 2889.
E-mail address: imato@cstf.kyushu-u.ac.jp (T. Imato).

http://dx.doi.org/10.1016/j.talanta.2014.10.055
0039-9140/

detection limit as low as IC_{80} of ca. 4 ppb [8]. To date, a combination of ELISA and an OLED and an OPD together for the determination of APE has not been reported.

The development of a downsized analytical system, such as a lab-on-a-chip (LOC) system and a micro-total analysis system (μ-TAS), has been an urgently sought subject in green analytical chemistry and has attracted the interest of many researchers as well as users of conventional analytical instruments. The LOC system and μ-TAS have many advantages, including high-analytical throughput, high portability, reduction in the time needed for an analysis, and a low consumption of reagents due to the fact that several analytical procedures are integrated into a centimeter sized chip. The intent of such systems is to miniaturize and to integrate an analytical laboratory onto a single chip (substrate) that can support several functions such as separation, concentration and detection for numerous applications in biochemistry and the life sciences. The integration of a light source and a photo-detector on a micro-fluidic chip is the key technology for fabricating a small optical system suitable for the LOC system and μ-TAS. In this case, microfluidic technologies based on an inorganic light emitting diode (LED) as the light sources are currently attracting considerable attention and appear to have increasing applications. The characteristics of such a system include small-size, low-cost, long lifetime, and low-power consumption compared to the currently used commercial instrumentation and household appliances [9–14].

In recent years, an OLED and an OPD are a promising light source and a photo-detector, respectively for fabrication of a small optical system on a micro-fluidic chip. Recently attempts to assemble an OLED or an OPD within monolithic substrates have been reported by several researchers [15–21]. Compared with common light sources like the inorganic LED and common photo-detectors, such as the charge coupled detector (CCD) and the photomultiplier tube (PMT), both the OLED and the OPD have a flat surface which makes it easy to integrate them into a microfluidic device. In addition to this, they are sufficiently flexible to be incorporated into any size and shape using photolithography techniques. For instance, Hofmann et al. reported on the use of a thin-film OLED which has a peak emission wavelength of 540 nm as an excitation source for microscale fluorescence detection. They fluorometrically determined human serum albumin (HAS) on a PDMS microchip containing 800 μm deep and 800 μm wide microchannels at a flow rate of 20 μL min^{-1}, and obtained a lower detection limit of ca. 10 mg L^{-1} [16]. We successfully combined an OLED with a CCD for a fluorometric immunoassay for immunoglobulin A (IgA) on a PDMS microchip [22], achieving a detection limit of 16.5 ng mL^{-1}. Compared with an immunoassay by using a conventional 96-well microtiter plate, the analysis time and the amounts of reagent and sample solutions could all be reduced [22]. On the other hand, several researchers have used an OPD instead of a CCD or a PMT as a photo-detector for chemiluminescence and fluorescence detection on microchip. For example, Hofmann et al. were the first group to report the effectiveness of using an OPD as an integrated optical detector for microscale chemiluminescence measurements. The OPD was used to monitor the chemiluminescence generated by a reaction of peroxyoxalate with a chemiluminescence reagent on a PDMS microchip. They obtained a good linear calibration curve between the concentration of peoxyoxalate and the chemiluminescence signal with a detection limit of ca. 1 mM and excellent reproducibility with R.S.D. below 1.5% [23]. We developed a flow fluorescence immunoassay for IgA on a PDMS microchip by combining a commercial green inorganic LED and a fabricated OPD, where resorufin, produced by an enzymatic reaction of Amplex Red and H_2O_2 with an HRP-labeled antibody was detected. The detection limit of 16 ng mL^{-1} for IgA was obtained [24].

However, only a few studies of a fluorometric immunoassay using a fluorescence detector combined an OLED with an OPD on a microchip have been reported. A fluorescence detector combined with an OLED and an OPD has many advantages, such as compactness, inexpensive, ease of fabrication onto any substrate, because the devices are flat, thus making them suitable for assembly on a flat shaped microchip. We report herein on an attempt to develop an integrated fluorescence detection system on a microchip by using an OLED with a narrow emission band as a light source and an OPD as a photo-detector. We selected a terbium complex as the emitting layer so as to obtain a narrow emission band for the OLED, while we fabricated the OPD based on the bulk heterojunction of n-type and p-type semiconductive materials to obtained a high IPCE instead of the OPD based on multiple layers of n-type and p-type semiconductive materials. The performance of the fluorescence detector assembled with the OLED and the OPD was evaluated for the detection of resorufin solutions. Finally the fluorescence detector was successfully applied to a competitive immunoassay for APE.

2. Experimental

2.1. Materials and chemical reagents

The materials used for the fabrication of the OLEDs and OPDs, 4,4′-bis[N-(1-naphthyl)-N-phenyl amino]-biphenyl (α-NPD), 4,4′-di (N-carbazolyl)biphenyl (CBP), m-bis(N-carbazolyl)benzene (mCP), terbium(acetylacetonato)$_3$(bathophenanthroline) (Tb(acac)$_3$bath), bathocuproine (BCP) and aluminum tris(8-hydroxyquinoline) (Alq_3) were obtained from Tokyo Kasei Co., Ltd., (Tokyo, Japan) and were used without further purification. Copper phthalocyanine (CuPc) and TPTPA obtained from Tokyo Kasei Co., Ltd., (Tokyo, Japan), were purified by three sublimations and used as a p-type semiconductive material. Fullerene 60 (C_{60}) and C_{70} with a purity of 99.95% were obtained from Material Technologies Research Ltd. (OH, USA) and used as received as an n-type semiconductive material. Molybdenum trioxide (MoO_3) was purchased from Strem Chemicals (Tokyo, Japan). A layer of indium tin oxide (ITO) deposited glass plate (thickness of the ITO layer, 110 nm) with the 7-stripes pattern was purchased from Sanyo Vacuum Industries Co., Ltd. (Osaka, Japan) and was cut at a size of 25 mm × 25 mm square (patterns size: stripes of 2 mm width and 23 mm length).

The PDMS microchip was fabricated using Sylgard 184 Silicone Elastomer Kit (Dow Corning Corporation) containing a base agent (a mixture of silica and tetra(trimethyl)siloxysilane) and a curing agent (a mixture of silica and octamethylcyclotetrasiloxane). A peek tube (0.125 mm i.d., 0.159 mm o.d.) was obtained from Upchurch Scientific Inc. (WA, USA).

All reagents used were of analytical reagent grade. Hydrogen peroxide (H_2O_2, 30% aqueous solution), APE, bovine serum albumin (BSA, Cohn Fraction V), N-hydroxysuccinimide (NHS), 1-ethyl-3-(3-dimethylaminopropyl) carbodiimide hydrochloride (EDC), tris (hydroxymethyl)aminomethane (Tris), sodium hydroxide (NaOH), and hydrochloric acid (HCl) were purchased from Wako Pure Chemical Industries Ltd. (Osaka, Japan). Tween 20 and glycine (Gly) were obtained from Kishida Chemical Co. Ltd. (Osaka, Japan). HRP-APE, the anti-APE antibody were received from Tokiwa Chemicals Industries Co. (Osaka, Japan). Amplex Red was purchased from Fluka Co. Ltd. (Tokyo, Japan) and resorufin was obtained from Sigma-Aldrich (Osaka, Japan). An aqueous suspension of magnetic microbeads coated with polylactic acid (average diameter: 100 μm) was purchased from Micromod Co. (Germany). Deionized water was purified by a Milli-Q water purification system (Millipore Co.) and used for preparation of all solutions.

2.2. Fabrications of the OLEDs and OPDs

Two types of green OLEDs (device A and device B) were fabricated on the ITO coated glass substrates by a multilayer thermal

evaporation method using a vacuum evaporation system (E-110, ALS Technology, Japan), as described in previous papers [22,25,26]. The structures of the two OLEDs fabricated in this work are as follows:

(device A) ITO (110 nm)/α-NPD (30 nm)/CBP:Tb(acac)$_3$bath (8 wt%, 30 nm)/BCP (30 nm)/Alq$_3$ (25 nm)/MgAg (100 nm)/Ag (50 nm).
(device B) ITO (110 nm)/α-NPD (30 nm)/mCP:Tb(acac)$_3$bath (8 wt%, 30 nm)/BCP (30 nm)/Alq$_3$ (25 nm)/MgAg (100 nm)/Ag (10 nm).

In order to compare the sensitivity of the preparations to light and optimize the performance of the present optical system, seven different kinds of OPDs (device A–G) were fabricated on ITO patterned glass substrates in the same manner as that for the OLEDs by a multilayer thermal evaporation method using the vacuum evaporation system, as described in our previous papers [8,24]. In the fabrication process the deposition rate was 0.02–0.05 nm s^{-1} under a pressure of $< 4 \times 10^{-4}$ Pa. The structure of the device G, which is used in this work, is as follows (the other devices' structures of the OPDs are shown in supplemental information):

(device G) ITO (110 nm)/ MoO$_3$ (6 nm)/TPTPA:C$_{70}$ (10 wt%, 40 nm)/BCP (10 nm)/Ag (50 nm).

The numbers in parenthesis indicate the thickness of each deposited layer component. The colon in devices D, F and G indicates that the two organic components were deposited simultaneously and the weight percentage in the parenthesis is that of CuPc or TPTPA. The number of active pixels on one OPD and its area are the same as those of the OLEDs. All of the devices were finally sealed with a glass cover using a UV cured epoxy adhesive. The encapsulation was done in a nitrogen glove box (KK-011 AS-Extra, ALS Technology) after transferring the OLEDs and OPDs fabricated in the vacuum evaporation system to a nitrogen glove box, which is connected to the vacuum evaporation system, in order to protect the devices from air and humidity. The fabricated OLEDs and OPDs were stored in the dark until used.

2.3. Microchip design and fabrication

In this study, a microchip with a T- or a Y-shaped channel was prepared by using a template, which was fabricated by a conventional soft lithography technique [27]. Images of the microchips designed in this work are shown in Fig. 1(a) and (b). For the T-shaped channel, the width, depth and the length of the main linear channel (channel 1) were 1.5 mm, 80 μm and 40 mm, respectively. The other branch channel (channel 2) with a width of 1 mm was connected to channel 1 at a position 5 mm from the inlet. Detail of the preparation procedures is same as that described in our previous papers [8,24]. PEEK tubes (0.75 mm i.d., 1/16 in. o.d. 40 mm long) were connected to the two inlets and the outlet of the microchip with a silane-modified urethane resin adhesive (Epoclear, Konishi Co., Japan). A microchip with a Y-shaped channel shown in Fig. 1(b) was prepared using a polyacrylic resin by procedures described in our previous paper [7]. In this case the depth of the channel was 1 mm.

2.4. Experimental setup and instrumentation

The schematic flow diagram for the fluorimetric immunoassay for APE using the optical detector assembled with the OLED and the OPD on the microchip is shown in Fig. 1(c). In this case, two different types of microchips were used. The first contained a T-shaped microchannel, as shown in Fig. 1(a), where the anti-APE antibody was immobilized on the surface of the microchip by a physical adsorption. The second contained a common Y-shaped microchannel, as shown in Fig. 1(b), in which the anti-APE antibody was immobilized on the magnetic microbeads were used. Photographs of the two microchips are shown in Supporting information Fig. S1(a) and (b) and an illustration and a photo of the optical system with the magnet to trap the magnetic microbeads on the microchip is shown in

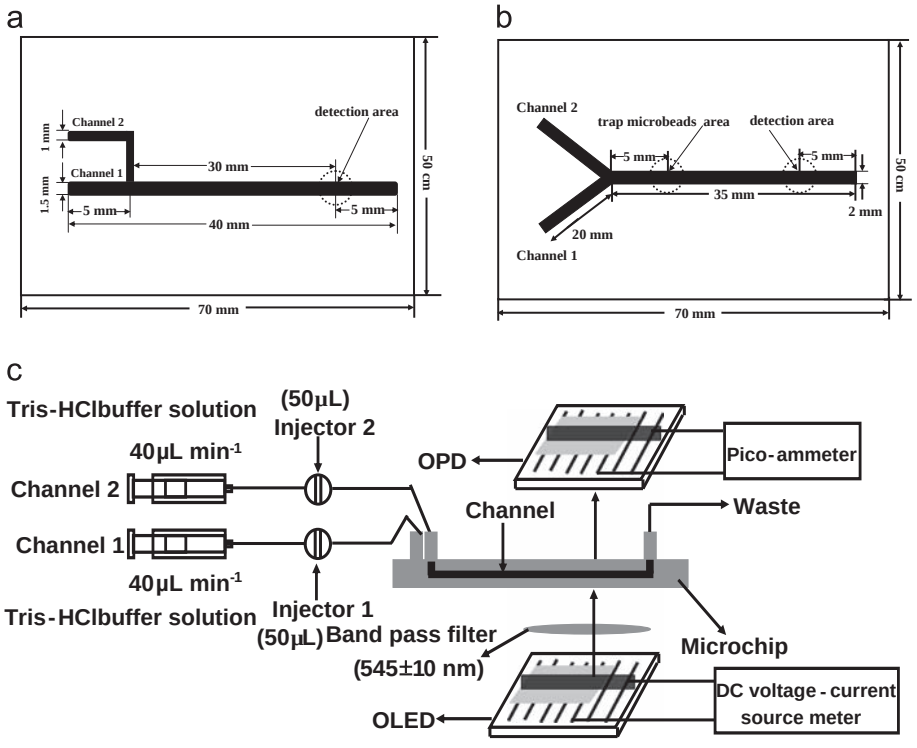

Fig. 1. (a) A microchip with a T-shaped channel for use in the physical immobilization of an antibody, (b) a microchip with a Y-shaped channel for use with magnetic microbeads containing an immobilized antibody and (c) schematic flow diagram of the optical system for the fluorometric immunoassay for APE. The depths of the T-shaped channel and the Y-shaped channel were 80 μm and 1 mm, respectively.

Fig. S1(c) and (d), respectively. As shown in Fig. 1(c), the OPD was placed directly on the microchip in order to adjust its position to the detection area of the flow channel in parallel to the microchip. The OLED was placed underneath the microchip in order to adjust its active pixels to the emission area of the flow channel to provide the excitation light for resorufin, a product of Amplex Red, produced by the enzyme reaction with HRP. In this case a band pass filter (545 ± 10 nm, Co. Ltd., Japan) was placed between the OLED and the microchip to eliminate the other emission bands of 545 nm from the OLED. The photocurrent from the OPD for the fluorescence light of resorufin generated by the enzyme reaction in the microchannel was measured by means of a picoammeter (6485, Keithley Instruments, Inc., OH, USA). A DC voltage–current source meter (6146, DC Instruments, Inc., Japan) was used to supply a constant current to the OLED. The intensity of the emission light from the OLED was controlled by the applied current of the source meter. A syringe pump system (NE-1002X, New Era Pump Systems Inc., NY, USA) with two syringes was used to pump the carrier solution into channel 1 and channel 2. Two injectors (9725, Rheodyne, CA, USA) were used to introduce the anti-APE antibody solution (or a suspension of the magnetic mirobeads containing the immobilized anti-APE antibody), the BSA solution, the mixed solution of the APE and HRP-labeled APE from injector 1 and the mixed solution of Amplex Red and H_2O_2 from injector 2.

The electroluminescence (EL) spectra of the OLEDs were recorded by using a multi-channel spectrometer (UBS2000, Ocean Optics). The current density (*J*)–voltage (*V*)–brightness (*B*) characteristics and external quantum efficiency (*EQE*) of the OLEDs were measured in ambient air with a semiconductor parameter analyzer (E5273A, Agilent) and an optical power meter (1930C, Newport).

In order to evaluate the performance of the fabricated OPDs, the OPDs were placed on a solar illumination stage and current–voltage curves (*JV* curves) in the dark and under a simulated AM 1.5 solar illumination (Otento-Sun II, KP type, Bunkokeik, Japan) with a Xe-lamp (Model XCS-150 A, Jasco, Japan) were obtained using a source meter (R6423, Advantest, Japan). The IPCE were calculated from the photocurrents of the OPDs, which were measured using the source meter under irradiation of a monochromatic light, which was generated by a Xe-lamp source (SK-U1152X, Ushio Inc., Japan) and a monochrometer (SM-10P, Bunkokeiki, Japan) from 400 nm to 800 nm at intervals of 10 nm. The incident light power of the monochromatic light was calibrated by using a Si photodiode (BS-520, Bunkokeiki, Japan) for calculating the conversion efficiency of the OPDs.

3. Results and discussion

3.1. Optimized the fundamental characteristics of the OLEDs and OPDs

The molecular structures of the emitting complexes and charge transport materials used for fabricating the OLEDs that are discussed in this paper are depicted in Fig. S2(a). In order to obtain the narrow band of the green emitting light for the excitation of resorufin, a rare earth metal complex, $Tb(acac)_3bath$ was used as the emitting complex. Since the host materials of the emitting complex have been found to influence the performance of the OLEDs [28,29], in order to optimize the fundamental characteristics of the present OLED based on $Tb(acac)_3bath$, two kinds of OLEDs were fabricated by using CBP and mCP as the host materials. For both OLEDs, the doping concentration of $Tb(acac)_3bath$ and the thickness of the emitting layer were the same, i.e., 8 wt% and 30 nm, respectively. Zhang et al. thoroughly investigated the effects of host materials and dopant materials in the emitting layer on the performances of OLEDs [28–31]. The PLQY of the emitting layer has a major influence on the efficiency of an OLED, so we anticipated that the EQE of devices based on Tb^{3+} complexes could be greatly improved by using a host material with a high triplet energy level. Indeed, for comparison, as shown in Table S1 in the Supporting information and in Fig. S3 of the Supporting information, the maximum EQE of device B composed of mCP was higher than that of the device A, composed of CBP. As we expected, when mCP was used as the host material, instead of CBP, the maximum EQE and maximum brightness of device B was 1.1% and 3029 cd m^{-2}, respectively. Both values are more than four times higher than the corresponding values for device A based on CBP as the host material.

It is generally known that, the photo-sensitivity of the OPD is dependent on the contacting surface area of the p- and n-type semiconductive materials and the absorptivity of light by the both conductive materials composed of the OPD. In our previous study [8,24], an OPD prepared by the vapor deposition of CuPc (p-type semiconductive material) and C_{60} (n-type semiconductive material) in a layered structure was used, as shown in Fig. S2(b). Zheng et al. reported that the IPCE of the OPD based on a bulk heterojunction of n-type semiconductive materials and p-type semiconductive materials (homogenous mixture of a n-type semiconductive material and a p-type semiconductive material) was higher than that based on a heterojunction with a layered structure [32–36]. The higher IPCE for the OPD based bulk heterojunction than that based on the layer by layer structure (Fig. S2(c)) may be due to the fact that the area of the interface between the p- and n-type semiconductive materials for a bulk hetrojunction is larger than that for a multi-layered structure. In this study, the maximum fluorescence spectrum of resorufin, the product of the enzymatic reaction of Amplex Red, was located at 586 nm, the IPCE of the previous OPD based on CuPc and C_{60} at 586 nm was 17.4%. In order to increase the IPCE of the OPD for a more sensitive detection of resorufin, p- and n-type semiconductive materials, which show a higher absorptivity to light at 586 nm can be used. Therefore seven kinds of OPDs were fabricated in an attempt to optimize the sensitivity to resorufin by using several p- and n-type semiconductive materials, as depicted in Fig. S2(b).

The performances of the OPDs, including *J*–*V* characteristics and IPCE spectra are shown in Fig. S4(b) and (c), respectively. The photovoltaic properties of the OPDs are summarized in Table S2. The highest values of the IPCE at around 500 nm and J_{SC} were obtained for the OPD fabricated from TPTPA and C_{70} with a bulk hetrojunction structure, where the concentration of TPTPA is 10%. These values for the OPD fabricated with the same bulk hetrojunction structure, where the concentration of TPTPA is 20% are lower than those for the OPD, where the concentration of TPTPA is 10%.

Based on the above results, in the following study, the OLED (device B), in which architecture is: ITO (110 nm)/α-NPD (30 nm)/mCP:$Tb(acac)_3bath$ (8 wt%, 30 nm)/BCP (30 nm)/Alq_3 (25 nm)/MgAg (100 nm)/Ag (10 nm) were used as the light source and the OPD (device G), the architecture of which is: ITO (110 nm)/TPTPA:C_{70} (10 wt%, 40 nm)/BCP (10 nm)/Ag (50 nm) were used as the photo-detector for the fluoresence determination of APE.

3.2. Evaluation of the light intensity of the OLED as a light source and the photosensitivity of the OPD as a photo-detector

The performance of the OLED as a light source used in the present work was evaluated by measuring the power of light emitted from the OLED (device B) by using the power meter (1918–C, Newport Co., CA, USA) at distance of 1 cm between the power meter and the OLED. The relationship between the power of the OLED and the applied current to the OLED is shown in Fig. 2(a). These data indicate that the light intensity from the OLED increases with increasing intensity of the applied current.

In order to evaluate the photosensitivity of the fabricated OPD as a photo-detector for the present work, the performance of the OPD was also evaluated by measuring the photocurrent of the OPD when the OPD was irradiated with light with different powers from a

conventional LED (maximum wavelength 545 nm). The power of the light from the LED was determined using a power meter and the present OPD by changing the distance between the LED and the power meter or the OPD (2–10 cm). Fig. S5(a) shows the relationship between the distance between the power meter and the LED and the LED power measured by the power meter based on a silicon diode. Fig. S5(b) shows the relationship between the distance between the OPD and the LED and the photocurrent measured by the OPD. The relationship between the photocurrent observed by the OPD and the power of the LED light irradiated to the OPD was obtained from data in Fig. S5(a) and (b). The results are shown in Fig. 2(b). This indicates that the photosensitivity of the present OPD is related to the light intensity at a certain wavelength.

3.3. *Performance of the fluorometric detector comprised of the OLED and the OPD for detecting resorufin fluorescence*

At the first stage of evaluation of the performance of the developed fluorometric detector, the response of the fluorometric detector showed in Fig. 1(c) to different concentrations of resorufin solutions, because resorufin is the enzymatic reaction product of Amplex Red and is intended to be used for the following immunoassay. In this case, the OLED (device B) was used as an excitation light source for resorufin. As can be seen from Fig. 3(a), the EL spectrum of the OLED is nearly identical to the PL spectrum of the $Tb(acac)_3$bath complex deposited onto the glass substrate and a maximum intensity in the EL spectrum of the OLED is observed at 546 nm, wavelength is overlapped well with the excitation spectrum of resorufin. This indicates that the present OLED is a suitable light source for the excitation of resorufin. However, since there are two low intensity emission peaks at around 575 and 625 nm, which are overlapped with the fluorescence wavelength of resorufin, the interference from these two emissions was eliminated by using a band pass filter.

For the detection of fluorescence from resorufin, the OPD (device G) was used in this case. As can be seen from Fig. 3(b), the IPCE of the OPD is 44% at the wavelength of resorufin (586 nm). This indicates that the fluorescence due to resorufin can be efficiently converted into a photocurrent by the present OPD. The photos of the OLED and the OPD are shown in the inset of Fig. 3(a) and (b), respectively.

The performance of the fluorescence detection system was evaluated by measuring the fluorescence of a series of resorufin solutions at different concentrations in a flow injection system shown in Fig. 1(c). In this case, the microchip with a T-shaped channel was used and only syringe pump 1 and injector 1 were used, while syringe

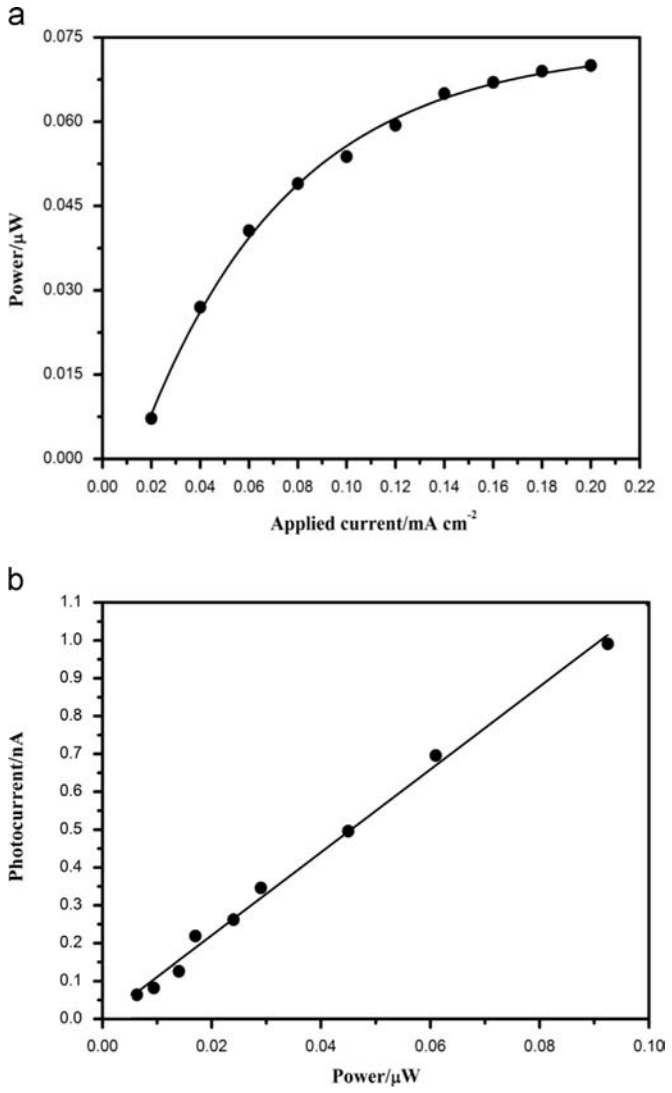

Fig. 2. (a) Relationship between the applied current to the OLED (device B) and the power of emitted light from the OLED measured by a power meter based on a silicon diode, (b) relationship between the photocurrent of the OPD (device G) and power of the light irradiated to the OPD from the conventional LED, which was measured by a power meter based on a silicon diode. The LED used for the light source has peak maximum of 545 nm (green light).

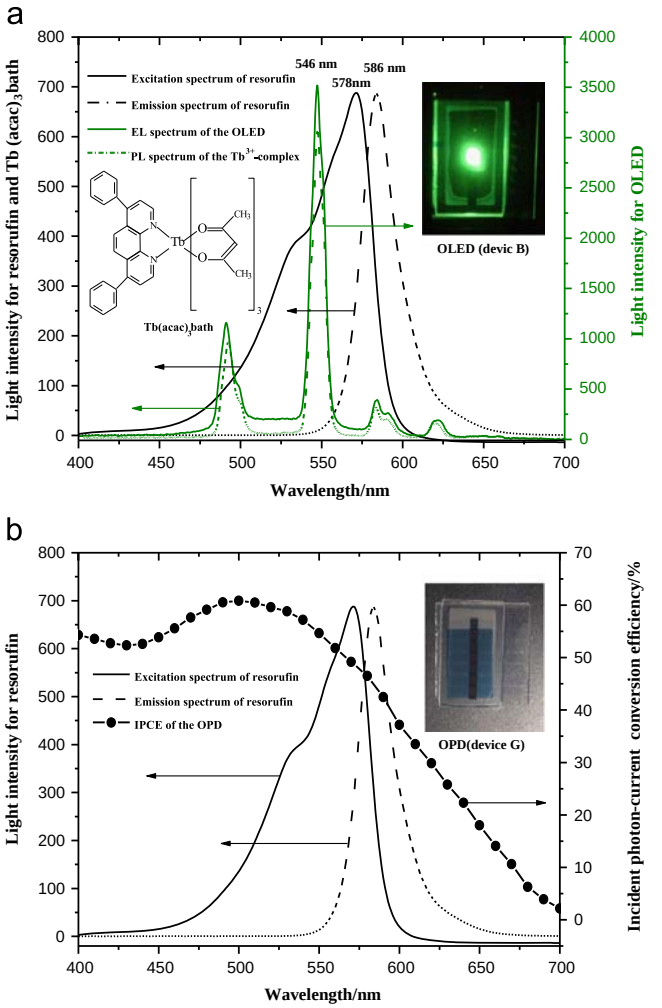

Fig. 3. (a) The PL spectrum of the $Tb(acac)_3$bath complex deposited on a glass substrate and the EL spectrum of the OLED (device B), and (b) the IPCE spectrum of the OPD (device G) and the excitation and emission spectra of the 10 μM resorufin solution. Inset illustrates the photographs of (a) the OLED and (b) the OPD.

pump 2 and injector 2 were not used. The inlet of channel 2 was sealed by a stop-plug. A 0.1 M phosphate buffer (pH=7.4) solution was used as the carrier solution and was pumped using syringe pump 1. In order to optimize the flow rate, the concentration of the resorufin solution and the injection volume were set at 18.7 μM and 50 μL, respectively and flow rates of 20 μL min^{-1} and 40 μL min^{-1} were examined. As shown in Fig. 4(a), when the flow rate was increased under the same injection volume (50 μL) condition, the detection time for a flow rate of 40 μL min^{-1} is shorter than that for 20 μL min^{-1}, however the peak height was almost the same. This result indicates that the dispersion of the injected sample is negligible and the time for passing the sample zone through the detection position is directly related to the flow rate. Under the same conditions, i.e., a flow rate of 40 μL min^{-1}, the peak signals obtained for the sample volume of 30 μL are smaller by about 15% than that for a volume of 50 μL. This indicates the sample injected at 30 μL is dispersed or diluted during its passage through the channel to the detector position. We chose the optimized condition at 50 μL for the injection volume and 40 μL min^{-1} for the flow rate in the following experiments.

In order to confirm the linearity of the photocurrent signals of the combined fluorometric detector against the concentration of resorufin, different concentrations of resorufin solutions were injected from injector 1, as shown in Fig. 1(c) under the optimized conditions. As shown in Fig. 4(b), trapezoid-shaped signals were obtained. An average of the photocurrent at the plateau of the signal (the period between 100 s and 200 s) was plotted against the concentration of resorufin and the data are shown in Fig. 4(c). A good linear relationship between the concentration of resorufin and the photocurrent was found and a detection limit (S/N=3) of 0.6 μM was obtained, with a correlation coefficient of 0.9978.

3.4. *Flow injection fluorometric immunoassay for APE by using the PDMS microchip immobilized with the antibody on its channel surface*

A competitive enzyme-linked immunosorbent assay for APE was performed on the PDMS microchip, where an anti-APE antibody was immobilized on the surface of the channel of the microchip, as shown in Fig. 1(a). The carrier solutions of the Tris–HCl buffer solution (pH=8.0) in syringes 1 and 2 were separately pumped and stopped depending on the protocol used. The flow rate of the both syringe pumps was set at 40 μL min^{-1}. The scheme and the enzymatic reaction of Amplex Red with HRP and H_2O_2 for the competitive immunoassay are shown in Fig. 5(a). First, a 50 μL aliquot of a 1 M NaOH solution and a 50 μL aliquot of a 1 M HCl solution were injected via injector 1 into the carrier stream of channel 1 at about 5 min intervals to wash the inside of the tube and the surface of the channel. Second, a 50 μL aliquot of a 1 mg mL^{-1} anti-APE antibody solution was injected from injector 1 into the carrier stream and, after 60 s, in order to maintain the

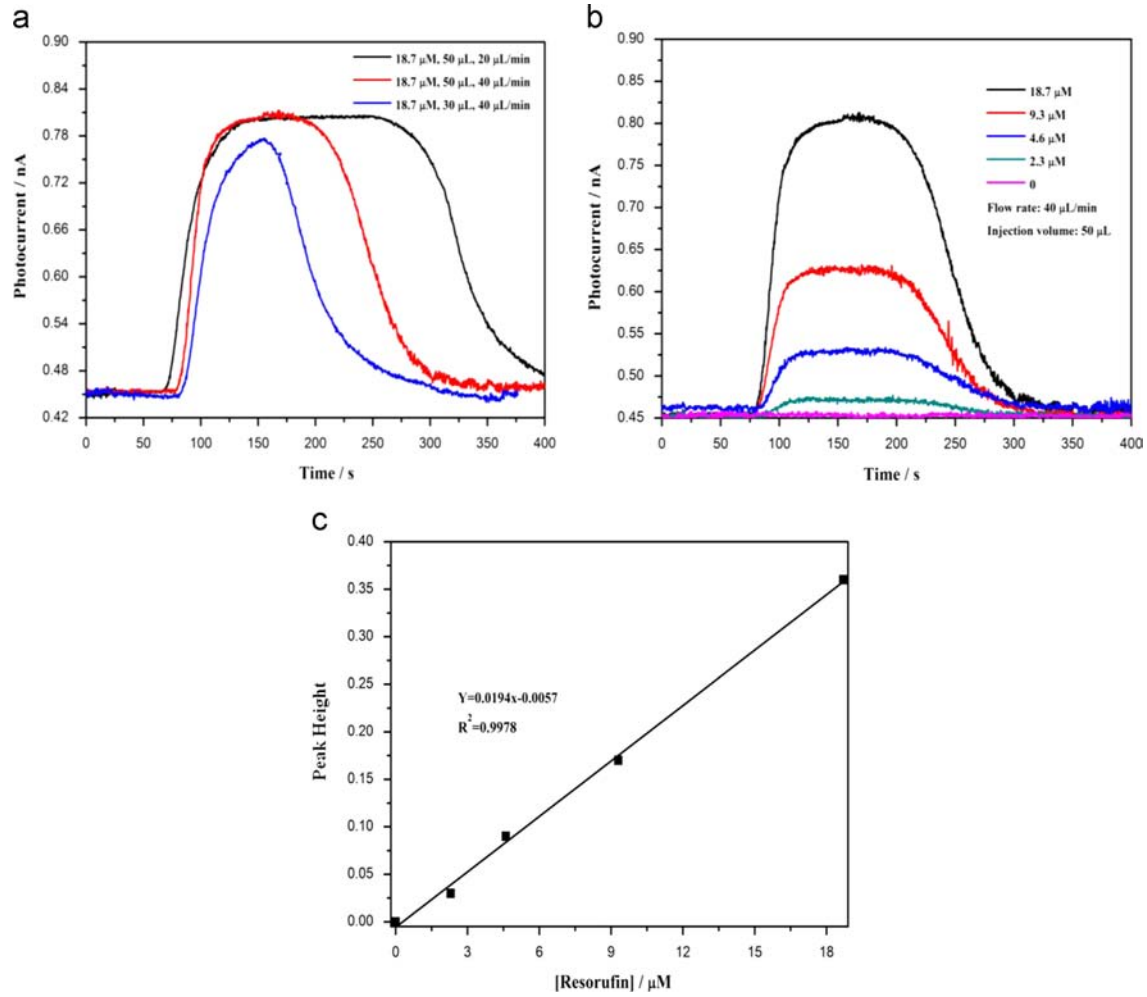

Fig. 4. Fluorescence response as photocurrent of the OPD to injections of resorufin solutions for investigating the effect of (a) injection volumes and flow rates under the constant resorufin concentration (18.7 μM), (b) concentration of resorufin under the constant flow rate (40 μL min^{-1}) and injection volume (50 μL), and (c) a calibration curve for resorufin based on the change in photocurrents.

antibody solution in the channel for the immunoreaction, syringe pump 1 was stopped for about 1.5 h. Third, the syringe pump 1 was re-started for about 10 min, to wash out the free antibody from the channel, and a 50 μL aliquot of a 10 mg mL^{-1} BSA solution was then injected from injector 1 to block the surface of the channel. After about 60 s, the syringe pump 1 was stopped for about 1 h to complete the blocking of the surface of the channel. Fourth, the syringe pump 1 was re-started for about 10 min to wash out the BSA solution from the channel, a 50 μL aliquot of a mixed solution of APE and the HRP-labeled APE was injected from injector 1 for about 5 min. The mixed solution consisted of 0–62.5 ppb APE and 500 ppb HRP-labeled APE. During the above procedures, syringe pump 2 was stopped. Finally, syringe pump 1 was stopped and syringe pump 2 was started, in order to inject a 50 μL aliquot of a mixed solution of 0.1 mM Amplex Red and 1 mM H_2O_2 from injector 2. After 1 min, syringe pump 1 was again started to flow the carrier solution. During flowing of the mixed solution of Amplex Red and H_2O_2 through the channel, where the anti-APE antibody complexes with APE and with HRP-labeled APE were immobilized, the enzyme reaction of Amplex Red and H_2O_2 with HRP of the HRP-labeled APE proceeds to produce resorufin. The fluorescence due to resorufin was measured by the optical system assembled on the microchip. The responses of the OPD as the photocurrent to the generated resorufin after injection of the mixed solution of Amplex Red and H_2O_2 are shown in Fig. 5(b). The photocurrent gradually increased at $t=50$ s and reached a maximum at around $t=100$–150 s and then gradually decreased, finally returning to the background photocurrent, which is due to the excitation light from the OLED. In this case, a calibration curve between the photocurrent normalized by the photocurrent observed for the blank solution and the APE concentration was obtained from Fig. 5(b). A typical sigmoidal calibration curve was obtained, as shown in Fig. 5(c). The detection limit defined as IC_{80} was ca. 1 ppb from the calibration curve. The analytical time for one sample was about 3 h. The present fluorometric immunoassay system would be

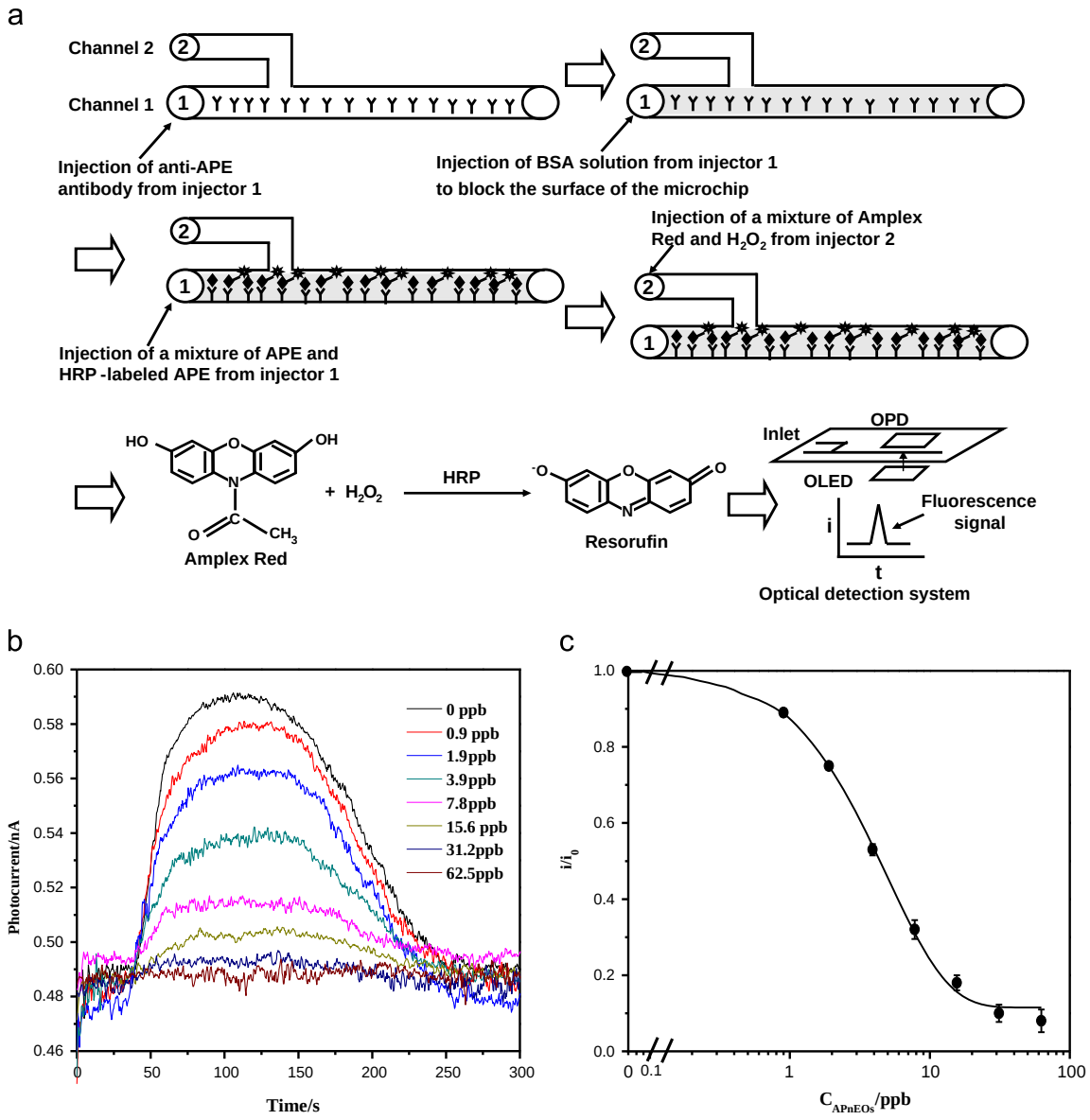

Fig. 5. (a) Schematic representation of the protocol for the competitive immunoassay for APE on the PDMS microchip immobilized with an anti-APE antibody on its surface, (b) fluorescence response of the OPD as photocurrent, when the mixed solution of Amplex Red and H_2O_2 was introduced into the microchip, where the enzyme reaction of Amplex Red with HRP-labeled APE proceeds and (c) calibration curve for APE by plotting the normalized photocurrent of the OPD by the photocurrent observed for the blank solution, the values at $t=125$ s of the response signal, against the concentration of APE.

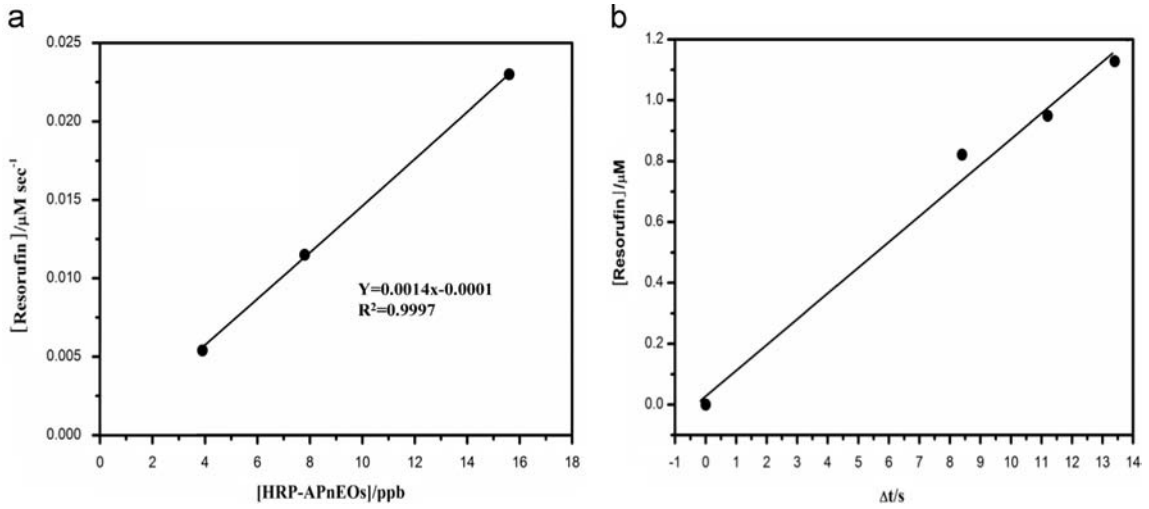

Fig. 6. (a) Relationship between the rate of the enzyme reaction and the concentration of the HRP-labeled APE, (b) a linear part of Fig. 6S (d).

satisfactory for the determination of APE in tap water samples judging from the lower detection limit and the regulation rules for Japanese Tap Water.

3.5. Estimation of the amounts of anti-APE antibody immobilized on the surface of the PDMS microchip

In order to estimate the amount of the anti-APE antibody immobilized on the surface of the PDMS microchip, the following experiments were carried out in a batch system and the flow system used in the previous immunoassay. Initially in the batch system, after 35 s from starting the monitoring of the fluorescence intensity, a 500 μL aliquot of different concentrations of an HRP-labeled APE solution (7.8–31.3 ppb) was quickly added to a quartz cell (1 cm path length) that contained, a 10 μL aliquot of a 10 mM Amplex Red solution and a 490 μL aliquot of a 2 mM H_2O_2 solution and the resulting solution was magnetically stirred. The final concentrations of the HRP-labeled APE, Amplex Red and H_2O_2 in the mixed solution were 3.9–15.6 ppb, 0.1 mM and 1 mM, respectively after the addition of the HRP-labeled APE solution. The fluorescence intensity at a wavelength of 586 nm (excitation wavelength: 576 nm) was monitored for the generation of resorufin in the quartz cell by the enzyme reaction of the HRP-labeled APE with Amplex Red and H_2O_2 for 600 s. The time-courses for the fluorescence intensity for three different concentrations of the HRP-labeled APE are shown in Fig. S6(a). As can be seen, the fluorescence signal rapidly increased to a maximum and then decreased to the baseline in the short time when the concentration of the HRP-labeled APE was 15.6 ppb. This may be due to fluorescence quenching at high concentrations. The slopes of the fluorescence intensity vs. time in a short time less than 5 s are related to the rate of the enzyme reaction. Indeed, there is a good linear relationship between the fluorescence intensity at 5 s and the concentration of the HRP-labeled APE, as shown in Fig. S6(b). Therefore, in order to determine the rate of the enzyme reaction, which is closely related to the HRP concentration, the relationship between fluorescence intensity of the resorufin solution and its concentrations (0.11–15 μM) was measured by means of a spectrofluorometer. The relationship is shown in Fig. S6(c). Using this relationship, the relationship between the rate of the enzyme reaction and the concentration of the HRP-labeled APE was determined, as shown in Fig. 6(a).

In order to estimate the total amount of the anti-APE antibody immobilized on the channel of the PDMS microchip, the same concentration of the anti-APE antibody (1 mg mL^{-1}) as was used in the immunoassay described in Section 3.4 was introduced into the channel. After immobilization of the anti-APE antibody, a 50 μL of 500 ppb HRP-labeled APE solution was introduced into the channel to form the immunocomplex of the anti-APE antibody with the HRP-labeled APE. A mixed solution of 0.1 mM Amplex Red and 1 mM H_2O_2 was then allowed to continuously flow into the channel at different flow rates and the effluent from the outlet of the channel was collected. The collected solution contained resorufin produced by the enzyme reaction of the HRP-labeled APE bound to the anti-APE antibody on the channel. The concentration of resorufin in the effluent is dependent of the average residence time in the channel, because the time of contact of the Amplex solution is dependent on the flow rate of its solution. The concentration of resorufin collected from the effluent was plotted against the average residence time in the channel and the results are shown in Fig. S6(d) and Fig. 6(b), respectively. There is a linear region between the concentration and the residence time in Fig. 6(b) and the slope of this linear region corresponds to the rate of production of resorufin in the channel. The amount of HRP-labeled APE bound to the channel can be estimated from the reaction rate calculated from the line shown in Fig. 6(b), by using the relationship between the reaction rate and the concentration of the HRP-labeled APE shown in Fig. 6(a). By taking into account the molecular weights of the HRP-labeled APE (ca. 40 kDa) and the anti-APE antibody (ca. 150 kDa) and the surface area of the channel (1.1 cm^2), it is possible to estimate the total amount of the anti-APE antibody immobilized on the channel and the results indicate that the amount is ca. 0.23 μg cm^{-2}. The surface density of the anti-APE antibody immobilized on the PDMS microchannel is comparable to that immobilized on the magnetic microbeads (1.3 μg g $beads^{-1}$), reported in our previous paper [7].

3.6. Flow injection fluorometric immunoassay for APE by using magnetic microbeads immobilized with the antibody on their surface

In order to compare the analytical results obtained by using the PDMS microchip, where the anti-APE antibody was immobilized on the surface of the microchip, an immunoassay method using magnetic microbeads as an immunosorbent that we proposed in a previous report [7,8], was applied to the fluorometric immunoassay using the optical system composed of the OLED and the OPD. The procedures for immobilizing the anti-APE antibody to the magnetic microbeads and the protocol for the immunoassay are shown in Fig. 7(a). The carboxyl groups on the magnetic beads were activated by using EDC and NHS, according to the protocol described in our previous report [8]. The anti-APE antibody was then covalently coupled with magnetic beads and the final product

was stored in 0.01 M pH=7.4 PBS with 1% BSA and 0.1% Tween at 4 °C. The illustration and the photograph of the optical system for the present immunoassay using the magnetic microbeads are shown in the Supporting information in Fig. S1(c) and (d), respectively. First, a 50 μL volume of the suspension of magnetic beads immobilized with the anti-APE antibody (2 mg mL^{-1}) was injected into the carrier stream, the flow rate of which was 40 μL min^{-1}, from injector 1 into the channel and the magnetic microbeads were trapped by a neodymium magnet (2 mm in diameter, Magfine Co., Japan), which was placed under the bottom of the microchip 5 cm downstream from the confluence point and shifted up and down by a solenoid. A 50 μL aliquot of a mixed solution of APE (0–62.5 ppb) and the HRP-labeled APE (500 ppb) was also injected into the microchannel from injector 1 and the carrier solution was allowed to flow for 5 min. During the above procedures, syringe pump 2 was stopped. Finally syringe pump 1 was stopped and syringe pump 2 was started permitting 50 μL of a mixed solution of Amplex Red and H_2O_2 to be injected into the microchannel from injector 2. Resorufin was produced during flowing of the mixed solution through the magnetic microbeads that were trapped in the channel by the enzyme reaction of HRP of HRP-labeled APE, which was bound to the anti-APE antibody on the magnetic microbeads. The fluorescence signal from resorufin was detected by the OPD. The fluorescence responses of the OPD as the photocurrent from the competitive immunoassay are shown in Fig. 7(b). The calibration curve for the fluorescence signal intensity normalized by the photocurrent observed for the blank solution plotted against the APE concentration is shown in Fig. 7(c). By comparing the calibration curve shown in Fig. 7(c) with that shown in Fig. 5(c), the shape of the both calibration curves is similar, but a

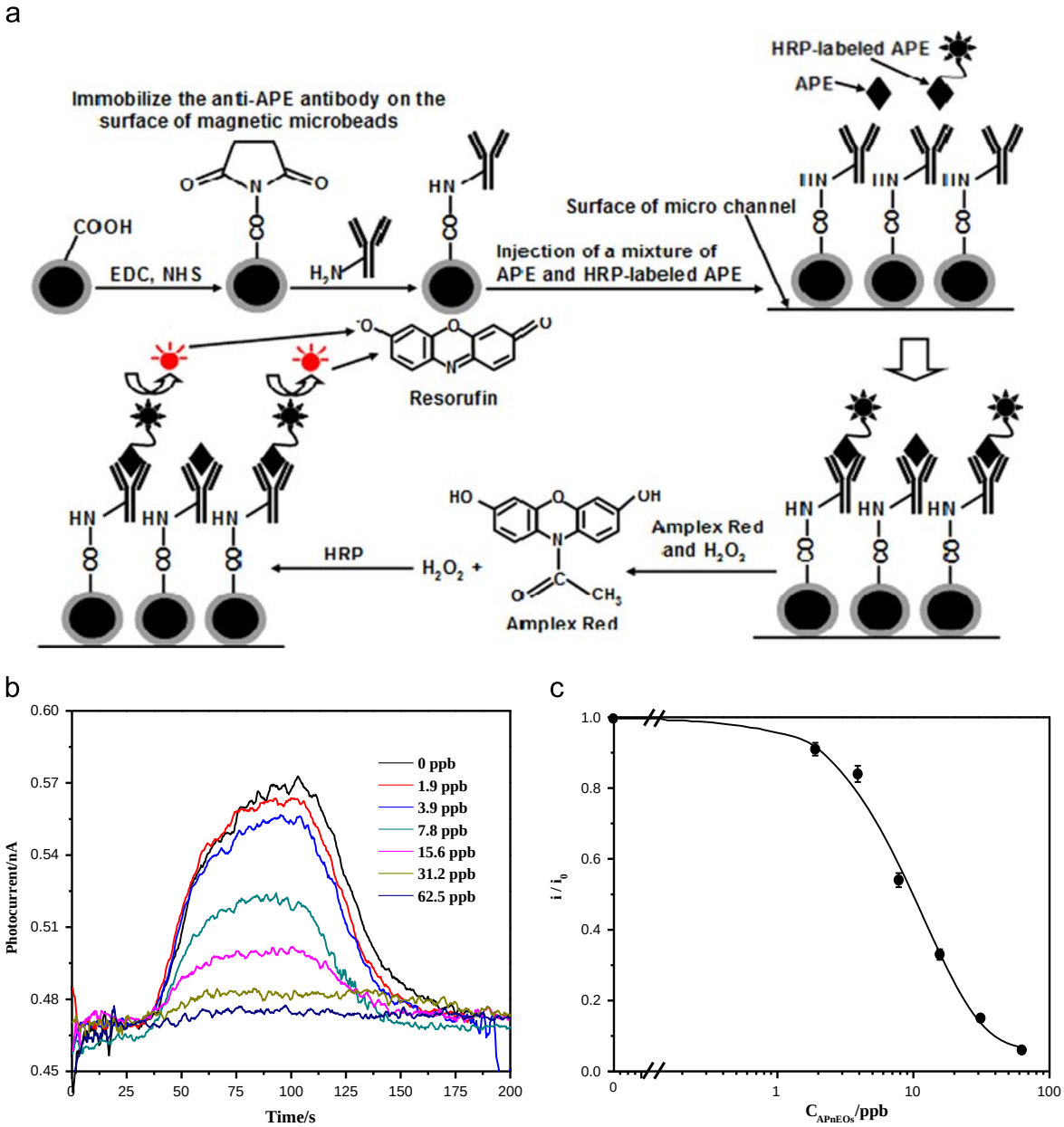

Fig. 7. (a) Schematic representation of the protocol for completive immunoassay by using microbeads immobilized with the anti-APE antibody on their surface, (b) fluorescence response of the OPD as photocurrent, when a mixed solution of Amplex Red and H_2O_2 was introduced into the microchip, where the enzyme reaction of Amplex Red with HRP-labeled APE proceeds and (c) calibration curve for APE obtained by plotting the photocurrent of the OPD, which is the value at t=100 s of the response signal, against the concentration of APE.

lower detection limit of 3 ppb was achieved when the magnetic beads were used, which is somewhat higher than that obtained using the PDMS microchip, where the anti-APE antibody is immobilized. An advantage of using the magnetic microbeads in the assay is that the total analytical time is substantially shorter, less than 10 min for one sample, while the analytical time for the other method is about 3 h for one sample. This is due to the fact that immunoreaction on the microbeads is faster than that on the PDMS microchip and the surface of the PDMS is relatively hydrophobic, therefore in order to protect the surface from absorbing molecules non-specifically, the blocking procedure by BSA is needed. In addition, the detection time for the fluorescence of resorufin obtained by the immunoassay where the anti-APE antibody was immobilized on the surface of the PDMS microchip was about 200 s from the photocurrent increase to return to the baseline, while the detection time for the fluorescence obtained by the immunoassay using magnetic microbeads was about 100 s. This may be due to the fact that the total area where the anti-APE antibody immobilized is wider for the case of immobilization onto the PDMS microchip, while the magnetic microbeads are trapped in a very small area. Furthermore, to compare of the lower detection limits (LODs) of our method with the relevant methods, as shown in Table S3, the LODs is in the order of our method based on fluorometric immunoassay < flow injection method based on fluorescence detector combined with LED and OPD using antibody immobilized magnetic beads [8] < sequential injection method based on chemiluminescence detector using antibody immobilized magnetic beads [7] < conventional ELISA method based on photometric detector [37].

3.7. Application of the present method to river water sample

In order to validate the present analytical method, we applied the present analytical system to the determination of APE in actual water sample, which is collected from a river in Fukuoka city at a distance of 300 m from the seashore. The collected sample solutions were filtrated through a membrane filter with the pore size of 0.45 μm and stored in a refrigerator at 4 °C. Since the original concentration of APE in the river water sample was lower than the detection limit of the present method, a standard solution of APE was added to the river water samples to adjust at 4 ppb as the final concentration. 22.5 mL aliquots of the river water sample was spiked by adding 2.5 mL of the 80 ppb standard APE solution, and the resulting solution was mixed with the HRP-labeled APE at the same volume. The recovery test was then carried out for the spiked samples according to the procedure described in Section 3.4. In this case, the FIA system shown in Fig. 1(a) and (c) was used for the determination of APE in river water sample and the results are shown in Fig. S7 and Table 1. R.S.D and recovery of 5.2% and 104 ± 3%, respectively, were obtained for the river water sample for 5 times measurements, as shown in Table 1. The good recovery of the present method comes from the highly selective immunoreaction of the anti-APE antibody with APE. This indicates that the present fluorometric immunoassay using the optical detector assembled with the OPD and the OLED is applicable to the real samples.

Table 1
Spike test of present method for river water samples.

Sample	Added (ppm)	Found (ppm)	R.S.D, % ($n=5$)	Recovery, % ($n=5$)
1#	4.00	4.12	5.2	104 ± 3%
2#	4.00	4.02		
3#	4.00	4.16		
4#	4.00	4.32		
5#	4.00	4.08		

4. Conclusion

We report on the development of an excellent and compact fluorometric detector by integrating an OLED based on a Tb^{3+}-complex co-doped with mCP as the light source and an OPD based on TPTPA co-doped with C_{70} as the photo-detector on a microfluidic microchip. The OLED based on the Tb^{3+}-complex co-doped with mCP as the emitting layer provides a narrow emission spectrum (an FWHM of 9 nm), and this type of light source is suitable for the selective determination of analytes. An OPD with a higher photosensitivity was developed by optimizing n-type and p-type semiconductive materials and using the bulk heterojunction of C_{70} and TPTPA instead of producing a layer upon layer structure. The performance of the fluorometric detector was evaluated by measuring the resorufin solution and a good linear relationship between the concentration of resorufin and the photocurrent of the OPD was found in the concentration range from 0 to ca. 20 μM and a lower detection limit ($S/N=3$) of 0.6 μM was obtained, with a correlation coefficient of 0.9978. Under the optimized flow conditions, the developed fluoromtric detector was applied to two kinds of competitive immunoassays for APE. One was performed using the PDMS microchip, where the anti-APE antibody was immobilized on the microchip, and the other was performed using the anti-APE antibody immobilized on magnetic microbeads. Typical sigmoidal calibration curves were obtained and the lower detection limits defined as IC_{80} were ca. 1 ppb and 2 ppb respectively for the above two methods. The latter immunoassay was found to be superior to the former, in that the analytical time was considerably shorter, about 10 min compared to hours. Due to the flat shape of the OLED and the OPD, they are suitable for insertion on a flat shaped microchip as a photometric detector as well as fluorometric detector. In the future we plan to fabricate flexible OPDs and OLEDs directly on a microchip.

Acknowledgments

This research was supported in part by the Japan Society for the Promotion of Science (JSPS) through its “Funding Program for World-Leading Innovative R&D on Science and Technology (FIRST Program)” and by JSPS KAKENHI Grant no. 25620117.

Appendix A. Supporting information

Supplementary data associated with this article can be found in the online version at http://dx.doi.org/10.1016/j.talanta.2014.10.055.

References

[1] R. White, S. Jobling, S. Hoare, J. Sumpter, M. Parker, Endocrinology 135 (1994) 175–182.
[2] E.J. Routledge, J.P. Sumpter, Environ. Toxicol. Chem. 15 (1996) 241–248.
[3] F. Ventura, A. Figueras, J. Caixach, I. Espadaler, J. Romero, J. Guardiola, J. Rivera, Water Res. 22 (1988) 1211–1217.
[4] A.D. Corcia, R. Samperi, A. Marcomini, Environ. Sci. Technol. 28 (1994) 850–858.
[5] C. Crescenzi, A.D. Corcia, R. Samperi, A. Marcomini, Anal. Chem. 67 (1995) 1797–1804.
[6] E. Engvall, P. Perlmann, Immunochemistry 8 (1971) 871.
[7] R.Q. Zhang, H. Nakajima, N. Soh, K. Nakano, T. Masadome, K. Nagata, K. Sakamoto, T. Imato, Anal. Chim. Acta 600 (2007) 105–113.
[8] R. Ishimatsu, A. Naruse, R. Liu, K. Nakano, M. Yahiro, C. Adachi, T. Imato, Talanta 117 (2013) 139–145.
[9] G.E. Collins, Q. Lu, N. Pereira, P. Wu, Talanta 72 (2007) 301–304.
[10] J.Z. Pan, B. Yao, Q. Fang, Anal. Chem. 82 (2010) 3394–3398.
[11] G. Ryu, J.S. Huang, O. Hofmann, C.A. Walshe, J.Y.Y. Sze, G.D. McClean, A. Mosley, S.J. Rattle, J.C. deMello, A.J. deMello, D.D.C. Bradley, Lab Chip 11 (2011) 1664–1670.
[12] F. Yang, X.C. Li, W. Zhang, J.B. Pan, Z.G. Chen, Talanta 84 (2011) 1099–1106.
[13] M. Ramuz, D. Leuenberger, L. Bürgi, J. Polym. Sci. 49 (2011) 80–87.

[14] S.H. Xue, K. Uchiyama, H.F. Li, J. Environ. Sci. 24 (2012) 564–570.
[15] B. Yao, G.A. Luo, L.D. Wang, Y.D. Gao, G.T. Lei, K.N. Ren, L.X. Chen, Y.M. Wang, Y. Hu, Y. Qiu, Lab Chip 5 (2005) 1041–1047.
[16] O. Hofmann, X.H. Wang, J.C. deMello, D.D.C. Bradley, A.J. deMello, Lab Chip 5 (2005) 863–868.
[17] B. Yao, H.H. Yang, Q.L. Liang, G.A. Luo, L.D. Wang, K.N. Ren, Y.D. Gao, Y.M. Wang, Y. Qiu, Anal. Chem. 78 (2006) 5845–5850.
[18] Y.H. Kim, K.S. Shin, J.Y. Kang, E.G. Yang, K.K. Paek, D.S. Seo, B.K. Ju, J. Microelectromech. Syst. 15 (2006) 1152–1158.
[19] C. Merfort, K. Seibel, K. Watty, M. Böhm, Microelectron. Eng. 87 (2010) 712–714.
[20] S. Kim, W. Choi, W. Rim, Y. Chun, H. Shim, H. Kwon, J. Kim, I. Kee, S. Kim, S.Y. Lee, J. Park, IEEE Trans. Electron Devices 58 (2011) 3609–3615.
[21] N. Misawa, S. Takeuchi, IEEJ Trans. Electr. Electron. Eng. 6 (2011) 97–100.
[22] H. Nakajima, Y. Okuma, K. Morioka, M. Miyake, A. Hemmi, T. Tobita, M. Yahiro, D. Yokoyama, C. Adachi, N. Soh, K. Nakano, S.H. Xue, H.L. Zeng, K. Uchiyama, T. Imato, J. Sep. Sci. 34 (2011) 2906–2912.
[23] O. Hofmann, P. Miller, P. Sullivan, T.S. Jones, J.C. deMello, D.D.C. Bradley, A.J. deMello, Sens. Actuators B 6 (2006) 981–987.
[24] M. Miyake, H. Nakajima, A. Hemmi, M. Yahiro, C. Adachi, N. Soh, R. Ishimatsu, K. Nakano, K. Uchiyama, T. Imato, Talanta 96 (2012) 132–139.
[25] B.H. Tanaka, T. Yasuda, K. Fujita, T. Tsutsui, Adv. Mater. 18 (2006) 2230–2233.
[26] W.G. Quirino, C. Legnani, R.M.B. dos Santos, K.C. Teixeira, M. Cremona, M. A. Guedes, H.F. Brito, Thin Solid Films 517 (2008) 1096–1100.
[27] D. Onoshima, J. Wang, M. Aki, K. Arinaga, N. Kaji, M. Tokeshi, S. Fujita, N. Yokoyama, Y. Baba, Anal. Methods 4 (2012) 4368–4372.
[28] Q.S. Zhang, T. Komino, S.P. Huang, S. Matsunami, K. Goushi, C. Adachi, Adv. Funct. Mater. 22 (2012) 2327–2336.
[29] Q.S. Zhang, J. Li, K. Shizu, S.P. Huang, S. Hirata, H. Miyazaki, C. Adachi, J. Am. Chem. Soc. 134 (2012) 14706–14709.
[30] M.A. Baldo, S.R. Forrest, Phys. Rev. B 62 (2000) 10958.
[31] R.J. Holmes, S.R. Forresta, Y.J. Tung, R.C. Kwong, J.J. Brown, S. Garon, M.E. Thompson, Appl. Phys. Lett. 82 (2003) 2422.
[32] Y.Q. Zheng, W.J. Potscavage, T. Komino, C. Adachi, Appl. Phys. Lett. 102 (2013) 153302.
[33] Y.Q. Zheng, W.J. Potscavage, T. Komino, M. Hirade, J. Adachi, Appl. Phys. Lett. 102 (2013) 143304.
[34] D. Yokoyama, Z.Q. Wang, Y.J. Pu, K. Kobayashi, J. Kido, Z. Hong, Sol. Energy Mater. Sol. Cells 98 (2012) 472.
[35] H. Ohishi, M. Tanaka, H. Kageyama, Y. Shirota, Chem. Lett. 33 (2004) 1266.
[36] G. Chen, H. Sasabe, Z. Wang, X.F. Wang, Z. Hong, Y. Yang, J. Kido, Adv. Mater. 24 (2012) 2768.
[37] Y. Goda, A. Kobayashi, S. Fujimoto, Y. Toyoda, K. Miyagawa, M. Ike, M. Fujita, Water Res. 38 (2004) 4323–4330.